IET Research Journals

IET Journals
The Institution of Engineering and Technology

Spectrally Efficient FDM over Satellite Systems with Advanced Interference Cancellation

ISSN 1751-8644
doi: 0000000000
www.ietdl.org

Hedaia Ghannam and Izzat Darwazeh FIET

Department of Electronic and Electrical Engineering, University College London, Gower Street WC1E 6BT, London, UK
** E-mail: hedaia.ghannam.15@ucl.ac.uk*

Abstract: For high data rates satellite systems, where multiple carriers are frequency division multiplexed with a slight overlap, the overall spectral efficiency is limited. This work applies highly overlapped carriers for satellite broadcast and broadband scenarios to achieve higher spectral efficiency. Spectrally efficient frequency division multiplexing (SEFDM) compresses subcarrier spacing to increase the spectral efficiency at the expense of orthogonality violation. SEFDM systems performance degrades compared to orthogonal signals, unless efficient interference cancellation is used. Turbo equalisation with interference cancellation is implemented to improve receiver performance for variable coding, compression and modulation/constellation proposals that may be applied in satellite communications settings. Such parameters may be set to satisfy pre-defined spectral efficiency values for a given quality index (QI) or associated application. Assuming LDPC coded data, the work proposes two approaches to receiver design; a simple matched filter approach and an approach utilising an iterative interference cancellation structure specially designed for SEFDM. Mathematical models and simulations studies are presented indicating promising gains to be achieved for SEFDM transmission with advanced transceiver architectures at the cost of increased complexity at the receiver.

1 Introduction

Given the scarcity of the available spectrum over satellite, coupled with the challenge to maximize satellite mass efficiency and transmit with high data rates in broadband and broadcasting applications, three main aspects for the system efficiency are to be improved: i) Payload mass efficiency through sharing the satellite's transponder by multiple carriers; ii) bandwidth efficiency by packing subcarriers closer to each other and using high-order modulation schemes; iii) power efficiency by operating the high power amplifier (HPA) close to its saturation region. For the first two aspects, interference avoidance has been the dominant paradigm in the design of conventional satellite communication systems to ensure that a simple receiver structure can effectively recover the transmitted information [1]. Frequency division multiplexing (FDM) is used in current satellite broadcast standards [2] to seperate subcarriers in frequency, where the number of subcarriers is limited (4 to 6) per transponder [3]. For a more efficient use of bandwidth, overlapping in the frequency domain is allowed while maintaining orthogonality between subcarriers. An example of overlapping frequency domain signals is orthogonal frequency division multiplixing (OFDM), where the spacing between the subcarriers must be set equal to the symbol rate of the information transmitted on each subcarrier [4]. To improve the satellite system efficiency, recent research has shifted its focus towards the interference management and exploitation paradigm [3]. In these systems, interference is no longer avoided, but intentionally introduced and mitigated by the use of specially designed transceiver architectures. The recent report of [5] derives an expression which shows that non-orthogonal multi-carrier signals have the potential to achieve higher capacity limits compared to Nyquist signals. Non-orthogonal signals with higher capacity are promising for future communication systems, especially in bandwidth-limited applications, such as satellite.

A marked contribution of improving spectral efficiency was proposed in 1975 by Mazo [6], where it was proven that, in a single carrier scenario, a 25% gain in spectral efficiency can be achieved at the same bit error rate (BER) and energy per bit E_b. This can be extended to a multi-carrier system by getting the subcarriers closer while compromising the orthogonality, as proposed in 2003, for non-orthogonal multi-carrier signal format named spectrally efficient frequency division multiplexing (SEFDM) [7] that achieves spectral efficiency gains by packing the subcarriers closer (relative to OFDM), while compromising the orthogonality. The multi-stream faster than Nyquist (FTN) technique proposed in [8] [9], is SEFDM's time domain counterpart and has similar spectral efficiency gains with little error performance loss relative to OFDM. Another spectrally efficient technique combines SEFDM with FTN to what is termed "time-frequency packing", where the time and frequency spacing are chosen to maximize the spectral efficiency [10].

SEFDM symbols are generated in a similar manner to OFDM using modified IFFT structures [11], yet they require more complex receiver structures [12]. Despite the non-orthogonality, techniques generally used in wireless systems, such as channel coding, channel estimation and equalisation have been applied to SEFDM with modifications and have led to systems where significant spectral efficiency gains were demonstrated in experimental wireless [13], optical/mm-wave [14] and very high speed optical [15] test beds. The work in this paper is motivated by aiming to improve the spectral efficiency to that of OFDM and beyond.

Although this paper focuses on optimising satellite systems spectral efficiency and assumes the system is operating in the linear region of the amplifier, it is important to emphasise that interesting results in [16] showing SEFDM exhibits lower peak to average power ratio (PAPR) compared to OFDM and that the PAPR of SEFDM decreases by increasing bandwidth compression. Thus, the possibility of SEFDM signal to reach the saturation region of the HPA is lower than that of OFDM and this is considered as an extra advantage. Furthermore, SEFDM promises to provide increased spectral efficiency at least for low-order modulation formats. Improving the achievable spectral efficiency without increasing the number of rings in the constellation amplitude phase shift keying (APSK) can be considerably convenient, since it is well-known that low-order constellations are more robust to channel impairments such as time-varying phase-noise and non-linearities [1].

In digital video broadcasting for satellite second generation (DVB-S2) [17], variable coding and modulation (VCM) is commonly applied to optimise the spectral efficiency and provide different levels of error protection to different service components (e.g. SDTV and HDTV, audio, multimedia). DVB-S2 based on SEFDM provides more freedom in optimising the system by adding another variable to VCM to become variable coding, compression (packing) factor α and modulation (VCCM).

The inherent inter-carrier interference (ICI) of SEFDM signal creates an environment with substantial distortion that will be severely damaging if left uncompensated. The self-induced interference between subcarriers is conceptually similar to ICI in OFDM but with far more severity. Different algorithms are developed to overcome ICI, which provide suboptimal solutions with lower complexity compared to the optimal maximum likelihood sequence estimation (MLSE). For instance, after the substantial performance gains of turbo coding and decoding algorithms [18], maximum aposteriori (MAP) turbo equalisation with an iterative equalisation and decoding was proposed by Douillard *et al.* in [19]. Impressive performance is gained by the MAP equaliser for systems that suffer from inter-symbol interference (ISI), where soft information, in the form of prior probabilities, is iteratively exchanged between detection and decoding [19]. Alternative turbo equalisation methods were introduced for further complexity reduction, such as the work in [20], [21], which utilises linear equalisation with decision feedback. Other design philosophies used in MIMO [22] cancel the interference gradually in each iteration.

This paper presents a new framework for a multi-carrier scenario, in which the same satellite transponder is exploited to serve multiple users at the same time. Two approaches are investigated to remove ICI resulting from compressing subcarreirs, within a transponder. The first approach is a simple single-user matched filter receiver used as a classical simple solution. The second approach termed serial interference canceller (SIC) is inspired by the technique of [22], where the interference is estimated and subtracted gradually in each iteration. Through extensive simulations, it is shown that the proposed multi-carrier analysis and SIC technique can be used to remove ICI. Only one iteration of joint equalisation and decoding is sufficient to approach the ideal performance when feeding back correct decisions. Useful performance examples are illustrated, which include bandwidth-efficient multiple carriers with M-ary Phase Shift Keying (PSK) modulation, that are FEC-encoded with the powerful low-density parity check (LDPC) codes adopted in DVB-S2 satellite standard in [17] and its more recent extension DVB-S2X [2].

The outline of this paper is as follows; we start with a short introduction to SEFDM signals in section 2. Variable coding, compression and modulation (VCCM) is investigated in section 3 to optimise spectrum utilisation over different satellite applications. Section 4 describes the system model in general, then sections 5 & 6 discuss two different approaches investigated to cancel the interference at the receiver; simple single-user matched filter receiver and SIC, respectively. Through simulations, the efficacy of these two techniques is shown. Finally, conclusions are drawn in section 7.

2 SEFDM Waveform Basics

Let $\mathbf{z} = \{z_0, z_1, .., , z_{N-1}\}, \mathbf{z} \in \mathbb{C}^{N\times 1}$, be the complex baseband symbols of symbol duration T_s, to be modulated by SEFDM in a multicarrier multiplexing technique, then the k^{th} SEFDM-modulated signal can be expressed as

$$x_k(t) = \frac{1}{\sqrt{T}} \sum_{n=0}^{N-1} z_{k,n} \exp\left(j2\pi kn\triangle ft\right), \quad 0 \le t \le T \qquad (1)$$

where N is the number of subcarriers, T is the SEFDM signal duration and $\triangle f$ is the frequency spacing between subcarriers. The SEFDM signal duration T is equal to $N \times T_s$. In contrast to OFDM, the SEFDM subcarriers are not orthogonal and $\triangle f \times T = \alpha$, where $\alpha \in (0, 1]$ is the compression factor.

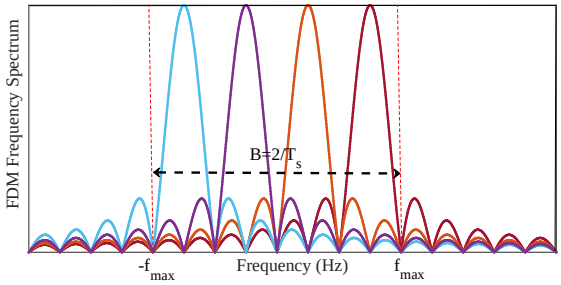

(a) FDM Spectrum

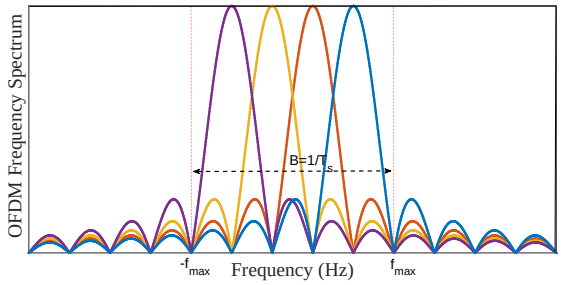

(b) OFDM Spectrum

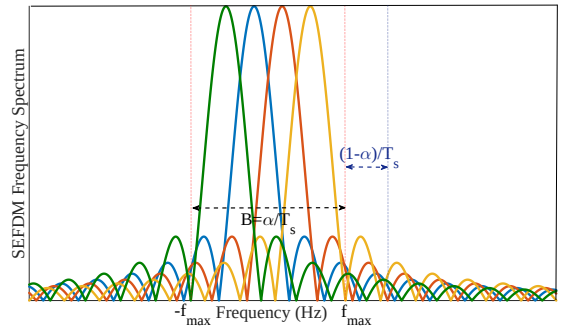

(c) SEFDM Spectrum

Fig. 1: A comparison of FDM, OFDM and SEFDM ($\alpha = 0.8$) spectra for the same bit rate and $N = 4$.

Consider the FDM, OFDM and SEFDM frequency spectra of the band-limited signal $x_k(t)$ in Fig. 1, for ideal time domain rectangular pulses of duration T. Clearly, OFDM in Fig. 1(b) occupies half of the bandwidth of FDM in Fig. 1(a), while SEFDM saves $(1-\alpha) \times 100\%$ bandwidth in comparison to OFDM for the same transmission speed. The violation of orthogonality is clear for the case of SEFDM in Fig. 1(c), as at the peak value of each subcarrier, other subcarriers are non-zero. To suppress the out-of-band power leakage of the SEFDM power spectrum in Fig. 1(c), Nyquist pulse shaping has been implemented in [23] as well as in a carrier aggregation scenario in [24].

Let $\hat{z}_{k,n}$ denotes the symbol estimate after matched filtering and used at the receiver side of OFDM, which is given in (2). The matched filter with symbol-by-symbol estimation, is no longer optimal for SEFDM, due to the ICI between subcarriers.

$$\hat{z}_{k,n} = \frac{1}{\sqrt{T}} \int_0^T x_k(t) \exp\left(-j2\pi kn\triangle ft\right)dt, \quad 0 \le n \le N-1. \qquad (2)$$

Following Nyquist, the signal is to be sampled at a minimum rate of ($f_s = 2f_{max} = B = \alpha/T_s$) to allow reconstruction of the signal from its samples at the receiver. Consequently, by sampling the signal in (1) at a regular interval of $\tau = T_s = T/N$, the total number of samples is $Q = T/\tau = N$. Therefore, $Q \ge N$ samples are required.

The sampled version $x_k(qT/N)$ of (1), or simply $x_{k,q}$ is

$$x_{k,q} = \frac{1}{\sqrt{Q}} \sum_{n=0}^{N-1} z_{k,n} \exp\left(j2\pi kn\triangle f \frac{qT}{N}\right) = \frac{1}{\sqrt{Q}} \sum_{n=0}^{N-1} z_{k,n} \exp\left(j2\pi k\alpha \frac{qn}{N}\right) \quad , 0 \le q \le Q-1 \quad (3)$$

where the factor $1/\sqrt{Q}$ in (3) is employed for normalization purposes [†]. Following the same method used to obtain (2), the discrete representation of the demodulated n^{th} data symbol of the k^{th} SEFDM symbol signal at the receiver side is given by [12]

$$\hat{z}_{k,n} = \frac{1}{\sqrt{Q}} \sum_{q=0}^{Q-1} x_{k,q} \exp\left(-j2\pi k\alpha \frac{qn}{N}\right) \quad , 0 \le n \le N-1. \quad (4)$$

Conceptually, the implementation of (1) and (2) may use a bank of modulators each tuned at a certain frequency. However, such generations are problematic because they require keeping a precise spacing between frequencies of subcarriers. In practice, they are implemented in the digital domain by means of IFFT and FFT, at the transmitter and receiver, respectively.

It is convenient to describe the transceiver process by a linear model. The transmitted signal in (3) can be expressed in a matrix form as [‡]

$$\mathbf{x} = \mathbf{\Phi z}, \quad (5)$$

where $\mathbf{x} = \{x_0, x_1, ..., x_{Q-1}\}$ is the vector of transmitted samples of $x(t)$ in (1) and $\mathbf{\Phi}$ is a $Q \times N$ matrix whose elements are given by

$$\Phi_{q,n} = \frac{1}{\sqrt{Q}} \exp\left(j2\pi\alpha \frac{qn}{N}\right) \quad 0 \le n \le N-1, 0 \le q \le Q-1. \quad (6)$$

Considering the signal is impaired by additive white Gaussian noise (AWGN), i.e., the noise samples w are identically and independently distributed with $zero$ mean and variance $\sigma_n^2 = N_0/2$, where N_0 is the noise power spectral density (PSD). Then, the received signal is

$$\mathbf{y} = \mathbf{\Phi z} + \mathbf{w}, \quad (7)$$

where $\mathbf{w}$ is a $Q \times 1$ vector, which represents the AWGN elements. The system model (7) is conventionally adopted in satellite systems, where in multi-carrier formats satellite-based physical layer modulation studies, the large scale variation and co-channel interference may be ignored since these are independent of the signalling format used [25] and with high power signal being sent along a line of sight channel, small signal variations are negligible as well. Next, the output of the FFT at the receiver is the estimate of the transmitted symbols given by

$$\hat{\mathbf{z}} = \mathbf{\Phi^H \Phi z} + \mathbf{\Phi^H w}, \quad (8)$$

where $(.)^H$ is the Hermitian operator used to obtain the complex conjugate of the modulation IFFT matrix $\mathbf{\Phi}$. In (8), if OFDM symbols are transmitted, then due to the orthogonality condition, the term $\mathbf{\Phi^H \Phi}$ turns into an identity matrix ($\mathbf{I}_N$) of size $N \times N$. Note that $\mathbf{\Lambda} = \mathbf{\Phi}^H \mathbf{\Phi}$, when $\alpha < 1$, has a diagonal of ones and non-diagonal elements ($\Lambda_{m,n}$) representing the correlation between two subcarriers m and n, which is given by [26]

$$\Lambda(m,n) = \frac{1}{Q} \sum_{k=0}^{Q-1} \exp\left(\frac{j2\pi m\alpha k}{Q}\right) \exp\left(\frac{-j2\pi n\alpha k}{Q}\right) = \frac{1}{Q}\left[\frac{1-\exp\left(j2\pi\alpha(m-n)\right)}{1-\exp\left(\frac{j2\pi\alpha(m-n)}{Q}\right)}\right]. \quad (9)$$

This matrix is of vital importance to the design of SEFDM receivers and it is worth noting that its elements are deterministic. In section 5, it will be shown that this prior knowledge can be exploited to mitigate the effect of ICI at the receiver. Given that α determines the spectral efficiency, the next section discusses how to adjust the spectral efficiency in satellite systems implementing SEFDM.

3 Variable Coding, Compression and Modulation

For a multi-carrier scenario, where a given transponder is exploited to serve multiple users simultaneously, SEFDM reduces the total occupied bandwidth or increases the throughput by increasing the number of users (subcarriers) per transponder. For example, in DVB-S2X standards, the maximum number of users per transponder is six [2]. Thus, if an SEFDM system with $\alpha = 0.8$ were to be used assuming the same coding and modulation order as in an OFDM system serving four users, then an SEFDM system would be capable of serving five users per transponder while maintaining the OFDM bandwidth or alternatively serve four users whilst saving 20% of the OFDM bandwidth.

DVB-S2/ DVB-S2X systems employing SEFDM may deliver broadcasting services over multiple transport streams, providing differentiated error protection (VCCM mode) to different service components (e.g. SDTV and HDTV, audio, multimedia). The lookup Table 1 (which may be stored in the memory of the transmitter) can be utilised to adjust the system parameters according to a given service quality index (QI). In this work, the modulation and coding examined are taken from the satellite standards DVB-S2 [17] and DVB-S2X [2], where eight different coding rates (R_c) are used with two constellation (M) levels (QPSK, 8-PSK). Here, we further examine the use of seven SEFDM compression factors. Adapting the standard definition of spectral efficiency (η) bit/s/Hz, as in the DVB standards [17], to account for the compression factor α, η becomes

$$\eta = \frac{\log_2(M) \times R_c \times R_s}{\alpha \times B}, \quad (10)$$

where R_s is the symbol rate and B is the OMUX bandwidth. A question that may be raised is: Instead of bandwidth compression, why not increase M or reduce R_c to achieve a better spectral efficiency? To validate the main argument of this paper and show the usefulness of SEFDM, extensive simulations are carried out for each group in Table 1 where the BER performance is compared to indicate the best VCCM. Four different signal groups are studied for scenarios where, in each group, the SEFDM signal occupies smaller bandwidth than that of an OFDM signal, therefore, the SEFDM and OFDM signals studied have the same spectral efficiency.

In the following, the transceiver system model used is explained in detail.

4 System Model: Transmitter

Consider the SEFDM system architecture depicted in Fig. 2. At the transmitter, in the first stage, a stream of bits $\mathbf{b} \in \{0,1\}$ are encoded by the outer Bose–Chaudhuri–Hocquenghem (BCH) encoder followed by an LDPC inner encoder. The BCH encoder is used to correct sporadic errors made by the LDPC decoder. The QI specified at the transmitter sets the code rate. The encoded bits $\mathbf{c} \in \{0,1\}$ are interleaved by an external block interleaver ($\prod_{ext}$) with equivalent size of normal baseband (BB)-FEC frame size (64,800) bits [17].

[†] *For simplicity, the condition that indicates $Q \ge N$ is omitted in the subsequent discussion of this paper.*

[‡] *For simplicity, the index that indicates the SEFDM block (k) is omitted in the subsequent discussion.*

Table 1 Lookup table for mapping QI to compression factor, coding rate and modulation

Group (QI)	η (bit/s/Hz)	α	R_c	$\log_2(M)$
I	0.67	1.0	1/3	2
		0.75	1/4	2
II	1.8	1.0	9/10	2
		1.0	3/5	3
		0.67	3/5	2
III	2.25	1.0	3/4	3
		0.8	3/5	3
		0.89	2/3	3
		0.71	4/5	2
IV	2.7	1.0	9/10	3
		0.83	3/4	3
		0.67	3/5	3
		0.67	9/10	2

The interleaver ensures that the independence of $\mathbf{c}$ approximately holds for several turbo equalisation iterations at the receiver stage.

The encoded bits $\mathbf{c}$ of the BB frame are then mapped and modulated. The QPSK/ 8-PSK modulator maps each $\log_2 M$ bits to a symbol z from the M-ary symbol alphabet $Z = \{z_1, z_2, ..., z_M\}$, $z \in \mathbb{C}$ where $M = 4$ for case of QPSK and $M = 8$ for 8-PSK. The mapping considered here is taken from the DVB standards [2] [17], with the symbol alphabet of zero mean ($M^{-1}\sum_{j=1}^{M} z_j = 0$) and unity energy ($M^{-1}\sum_{j=1}^{M} |z_j|^2 = 1$).

The mapped symbols sequence $\mathbf{z}$ is then divided into N parallel streams. In DVB-S2X, the maximum number of subcarriers per transponder is six [2]. These may be divided into filtered groups [3] or taken as one group of subcarriers [27], where four FDM subcarriers are used per transponder. Here, we adopt similar specifications to [27], with four subcarriers, but we apply OFDM and SEFDM modulation characteristics. Each parallel stream is modulated onto SEFDM subcarriers by means of an IFFT as shown in (3), where the QI defines the compression factor (α). We note that an illustrative SEFDM signal generation is represented in this block diagram, while the exact details of different methods for SEFDM signal generation are described in [11] and [13].

The sampled parallel output of the IFFT is multiplexed to $\mathbf{x}$, up-converted to the Ku frequency band (f_c GHz) using the in-phase and quadrature components (IQ) modulator to obtain the bandpass signal

$$\mathbf{x}_T = \Re\{\mathbf{x}e^{j2\pi f_c t}\}. \tag{11}$$

Subsequently, the real modulated stream of the SEFDM symbols $\mathbf{x}_T$ goes through the input multiplexer (IMUX) filter to select the desired group of N subcarriers and limit the interference with adjacent subcarriers. The IMUX output is then amplified by an HPA and finally, filtered again by the output multiplexer (OMUX) filter at the far end of the gateway to limit the interference to neighbouring subcarriers before $\mathbf{x}'_T$ is transmitted over the satellite downlink channel. For simplicity, the HPA is assumed to operate in its linear region as assumed by other work of [28]. The IMUX, OMUX and HPA transfer characteristics are also assumed to be ideal, since the standards (H.7) in [17] consider linearized HPAs and a highly selective IMUX and OMUX filters.

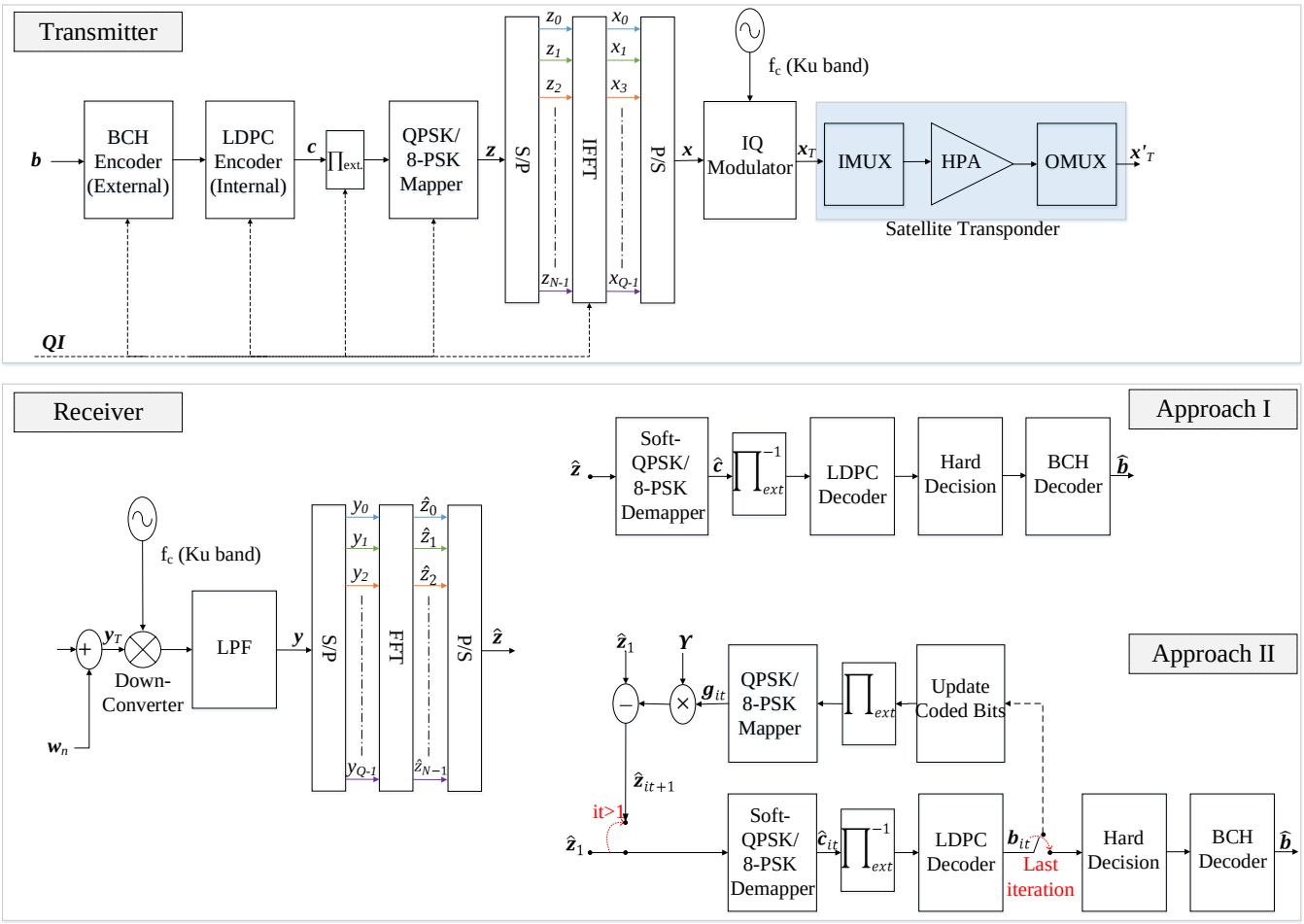

Fig. 2: Transceiver block diagram.

5 System Model: Receiver

At the receiver of Fig. 2, the first stage down-converts the received bandpass signal $\mathbf{y}_T$ to its baseband complex equivalent $\mathbf{y}$, using a down-converter and a low pass filter (LPF) combination. To obtain estimates $\hat{\mathbf{z}}$ of the transmitted symbols, demodulation is then performed using matched filters by means of an FFT . Subsequently, the symbols estimates will be used to detect the message transmitted. In the sections below, two approaches are examined for the detector: The first approach is a classical single-user matched filter receiver and the second is based on SIC.

5.1 *Approach I: Single-User Matched Filter Receiver*

In the receiver section of Fig. 2, the block diagram of approach I shows the design for a classical receiver. In the first stage, the estimated symbols $\hat{\mathbf{z}}$ are demodulated by employing an approximate log-likelihood ratio (LLR) algorithm to obtain soft bit estimates $\hat{\mathbf{c}}$. Then, the soft bits are deinterleaved and the LDPC decoder decodes the deinterleaved soft bit values to generate hard decisions. Finally, the BCH decoder works on these hard decisions to create the final estimate of the received bits $\hat{\mathbf{b}}$.

The BER of this receiver is simulated for the case of DVB-S2 TV broadcasting. The signal and system parameters used are shown in Table 2. BER results are shown to compare the bandwidth saving SEFDM case to the Nyquist case OFDM. If FDM were to be used, the bandwidth savings advantage of SEFDM will be enhanced by at least a factor of 2, depending on α.

Table 2 Signal and system modelling parameters

Parameters	Value
Symbol rate	27.5 Msymbols/s
Symbol duration (T_s)	36.36 ns
SEFDM symbol size (N)	4
SEFDM symbol duration(T)	$N \times T_s$
Subcarrier Spacing	$\alpha/(N \times T_s) = \alpha \times 6.875$MHz
Satellite transponder bandwidth	$\alpha \times 27.5$MHz
Modulation format	QPSK; 8-PSK
Coding Rate	1/3; 1/4; 9/10; 3/5; 3/4; 2/3; 4/5
α	1; 0.75; 0.67; 0.8; 0.89; 0.71
LDPC decoder number of iterations	50
IC number of iterations	1

Fig. 3 shows the BER results versus energy per bit E_b over N_0 (E_b/N_0) in dB, using the single-user matched filter receiver described above with 50 LDPC decoder iterations for the different groups of Table 1. The minimum BER achieved in the simulations is 10^{-5}, which leads to approximately free packet error rate (PER) [17].

In the simulations to follow, to allow fair comparison for given values of spectral efficiencies, both the bit rate and occupied bandwidth were adjusted for each group and the results are shown in Fig.

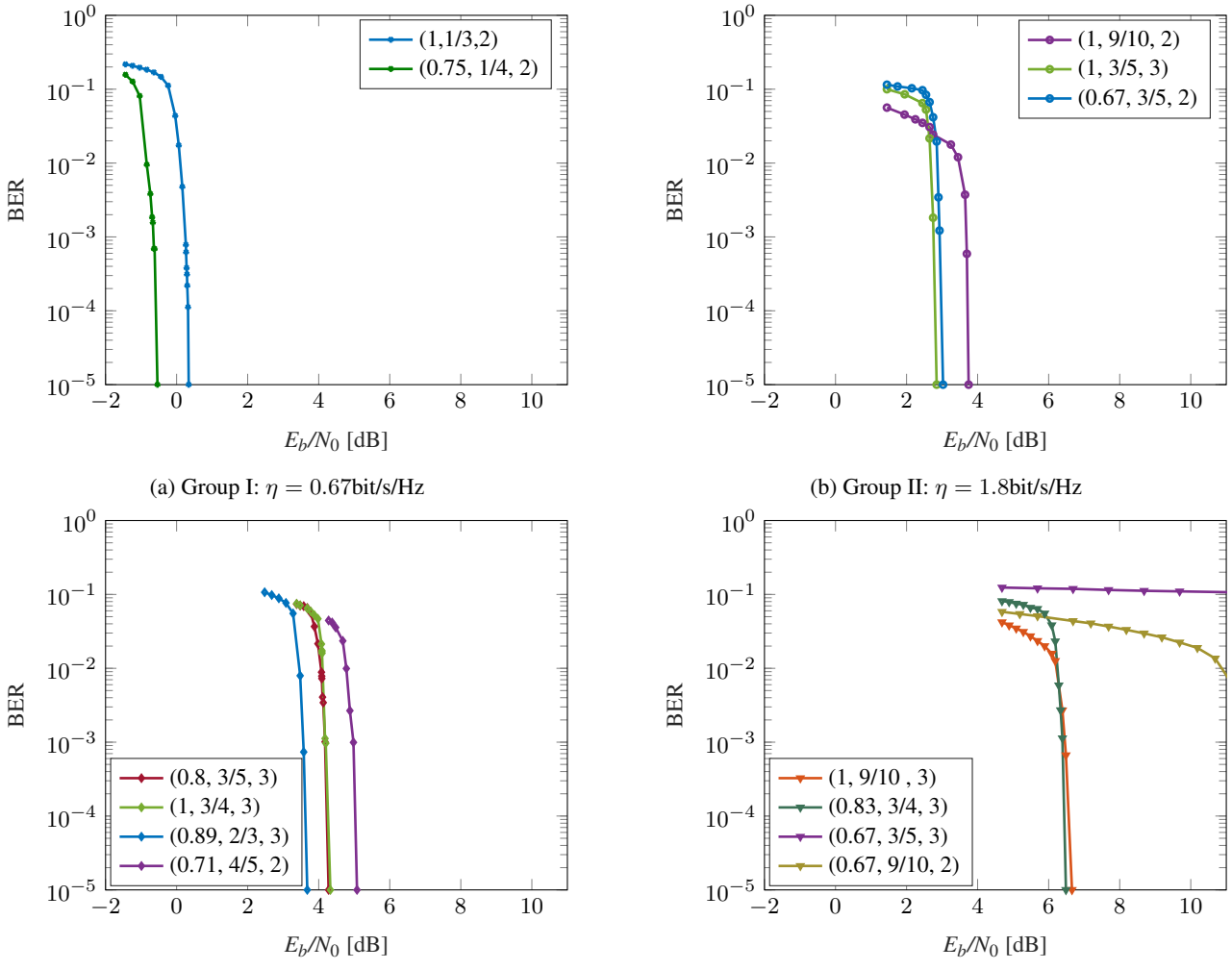

(a) Group I: $\eta = 0.67$bit/s/Hz

(b) Group II: $\eta = 1.8$bit/s/Hz

(c) Group III: $\eta = 2.25$bit/s/Hz

(d) Group IV: $\eta = 2.7$bit/s/Hz

Fig. 3: SEFDM system BER performance for the different QI groups with approach I receiver design and different VCCM parameters (α, R_c, $\log_2(M)$).

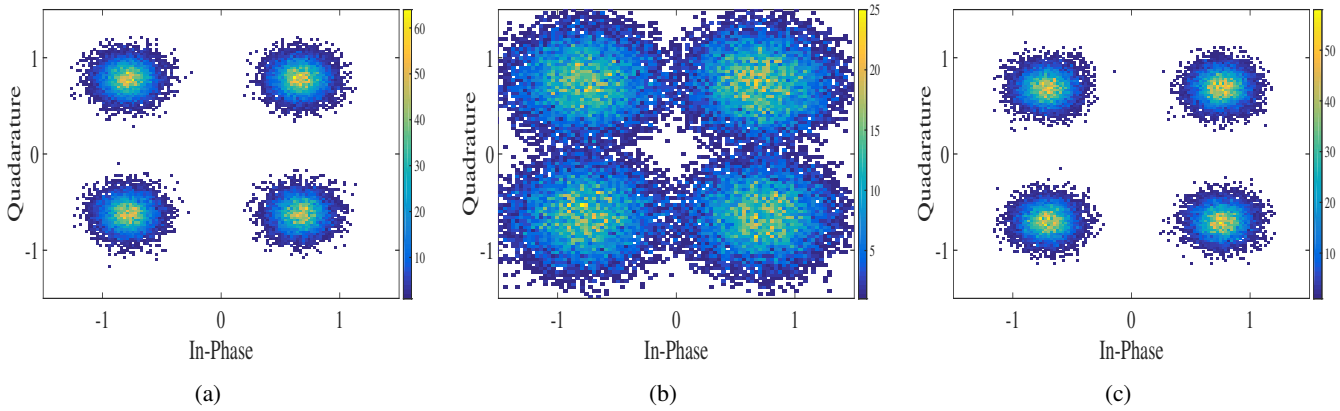

Fig. 4: The constellation diagram for the received QPSK symbols (a) OFDM, (b) SEFDM ($\alpha = 0.8$) before SIC iteration and (c) SEFDM ($\alpha = 0.8$) one SIC iteration.

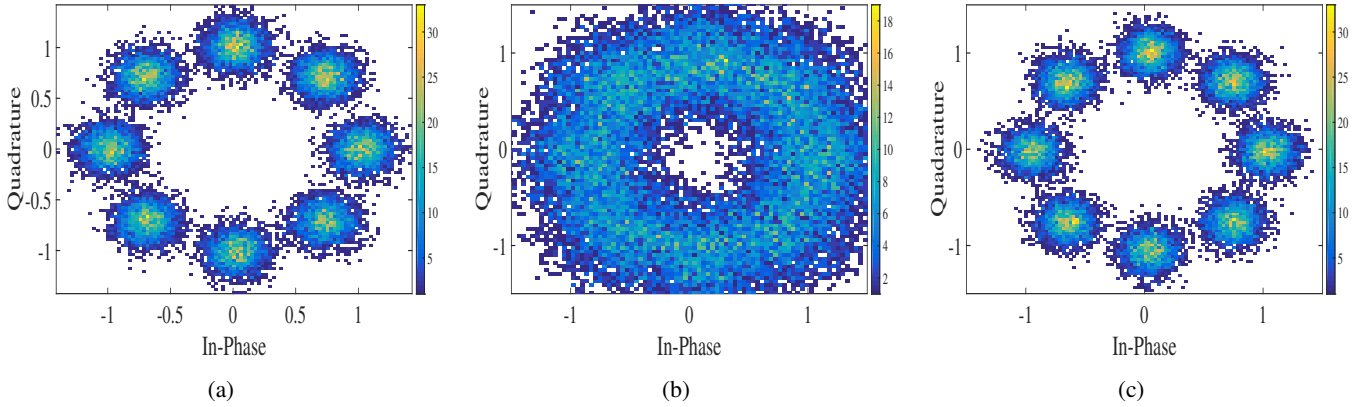

Fig. 5: The constellation diagram for the received 8-PSK symbols (a) OFDM, (b) SEFDM ($\alpha = 0.8$) before SIC iteration and (c) SEFDM ($\alpha = 0.8$) after one SIC iteration.

3. For clarity, the arrangement is held by subdividing the results according to the spectral efficiency (i.e. QI used), where the legend contains three values; α, R_c and $\log_2 M$, respectively. The first group ($\eta = 0.67$bit/s/Hz) in Fig. 3(a) shows the advantage of using SEFDM with a lower coding rate rather than OFDM, as 0.8dB power advantage is evident for the same BER performance, with a detector similar to what is typically used in multi-carrier satellite systems. This SEFDM scenario occupies 25% smaller bandwidth relative to an OFDM system with the same spectral efficiency.

The results of group II and III for higher values of η show that if the compression factor satisfies the Mazo limit (i.e. $\alpha \geq 0.8$), SEFDM slightly outperforms OFDM and with lower α there is no performance advantage of using SEFDM (e.g. Fig. 3(b)) in terms of power savings, although bandwidth savings are still guaranteed for the same spectral efficiency. Finally, for $\eta = 2.7$bit/s/Hz for group IV in Fig. 3(d), the system becomes more prone to ICI, thus, for α less than Mazo limit, the error floor is high and the system does not converge.

To conclude, SEFDM with a single-user matched filter receiver is beneficial, in terms of power saving, only for low η. To attain a system advantage, a more sophisticated receiver is required. Consequently, the following work approaches the problem from a different perspective; attempting to minimise the ICI effect through interference cancellation technique, by implementing a turbo equaliser and an SIC.

5.2 Approach II:Serial Interference Cancellation

In general, equalisation is used in communication systems to compensate for channel effects or other impairments that impact the received data. Equalisers estimate the transmitted symbols by filters whose parameters are selected using either linear, such as zero forcing (ZF) and minimum mean square error (MMSE) or non-linear processing, such as MLSE [20].

Soft-input soft-output (SISO) linear equalisers are dominant in many communication systems dealing with interference, such as sending a single-carrier signal in a multipath channel [20] or code division multiple access (CDMA) [21]. Potentially, this method would be expected to operate well in removing the interference of SEFDM. However, one of the limitations of SEFDM is the large condition number of its correlation matrix (9), which increases by reducing α [12]. Thus, SEFDM suffers with any equalisation method that requires matrix inversion. Alternatively, other interference cancellation methods subtract the ICI gradually instead of inverting its effect, which is considered in the following due to their suitability for SEFDM.

The design philosophy of SIC is based on an iterative process, which may be viewed as a synthesis of the processes used in [22] and for convolutional coded SEFDM in [14]. In this approach, the LDPC decoder outputs soft LLR values for the encoded bits, which are used to generate, through mapping and ICI estimation processes, approximate "replicas" of the received symbols, which in turn are used to cancel the interference, iteratively. The constellation diagrams of Fig. 4 and Fig. 5 show the effectiveness of SIC in reducing the ICI with only one turbo equaliser iteration for the case of $\alpha = 0.8$. Fig. 4 is for the case of QPSK, where the SEFDM constellation of (b) turns into (c) after one iteration and this constellation is similar to the interference-free case of OFDM (a). The same can be observed with Fig. 5 for the 8-PSK case.

The receiver implementation is shown at the bottom in Fig. 2 (Approach II), where the feedback processes are shown in dashed lines. At the first iteration ($it = 1$), the initial estimate vector $\hat{\mathbf{z}}_1$ is the same as what was shown before in (8). The LDPC decoder is fed by soft bits $\mathbf{c}_{it}$ from the soft demapper, where the index (it) indicates the iteration number. There are two outputs from the LDPC decoder; the soft LLRs of the encoded bits $\mathbf{c}_{it}$ used to update the encoded stream shown in the figure and the extrinsic LLR information (inside the LDPC decoder block and therefore not shown explicitly in the figure) that will be fed to the LDPC decoder as $a\ priori$ information in the next iteration. The updated encoded stream is mapped again via QPSK/ 8-PSK mapper to $\mathbf{g}_{it}$. The new estimate $\mathbf{g}_{it}$ of the transmitted symbols is then used to cancel the interference.

The non-diagonal elements of the cross correlation matrix $\mathbf{\Lambda}$ (9) represent the ICI between subcarriers in SEFDM systems and can be expressed by the $N \times N$ matrix $\mathbf{\Upsilon}$. By setting the diagonal of $\mathbf{\Lambda}$ to zeros using

$$\mathbf{\Upsilon} = \mathbf{\Lambda} - \mathbf{I}_N, \tag{12}$$

where $\mathbf{I}_N$ is an $(N \times N)$ identity matrix. The resulting interference canceler matrix $\mathbf{\Upsilon}$ is then multiplied by the estimated vector symbols $\mathbf{g}_{it}$ to evaluate the estimated ICI, given by the term $(\mathbf{\Upsilon} \times \mathbf{g}_{it})$. The estimated ICI is subtracted from the initial estimates $\hat{\mathbf{z}}_1$, as stated in (13), to give $\hat{\mathbf{z}}_{it+1}$, which forms the input to the next iteration.

$$\begin{aligned} \hat{\mathbf{z}}_{it+1} &= \hat{\mathbf{z}}_1 - \mathbf{\Upsilon}\hat{\mathbf{g}}_{it} \\ &= \hat{\mathbf{z}}_1 - (\mathbf{\Lambda} - \mathbf{I}_N)\hat{\mathbf{g}}_{it} \\ &= \hat{\mathbf{z}}_1 - \mathbf{\Lambda}\hat{\mathbf{g}}_{it} + \hat{\mathbf{g}}_{it}. \end{aligned} \tag{13}$$

For clarification, consider the case of the first iteration, where the input to the SIC turbo equaliser is the output of the receiver FFT $\hat{\mathbf{z}}_1$ given in (8). By substituting $\hat{\mathbf{z}}_1$ in (13)

$$\hat{\mathbf{z}}_2 = \hat{\mathbf{g}}_1 + \mathbf{\Lambda}(\mathbf{z} - \hat{\mathbf{g}}_1) + \mathbf{\Phi}^H \mathbf{w}. \tag{14}$$

The second term on the right hand side of (14) represents the difference between the transmitted symbols $\mathbf{z}$ and the estimated $\mathbf{g}_1$, hence, by getting a better estimate this term becomes smaller. After the last iteration, a hard decision is made on the output of the LDPC decoder and the BCH decoder in the final stage estimates the transmitted information bits $\hat{\mathbf{b}}$.

The system advantage of using SIC becomes evident when considering the BER performance for SIC approach, which is tested for the same parameters of approach I, with results shown in Fig. 6. The advantage of SEFDM over OFDM with one SIC iteration for the same η is clear for the four different groups. SEFDM saves bandwidth compared to OFDM and requires less power while maintaining the same BER performance. For instance, a 33% bandwidth and 2.8dB power savings are guaranteed for group IV ($\eta =$

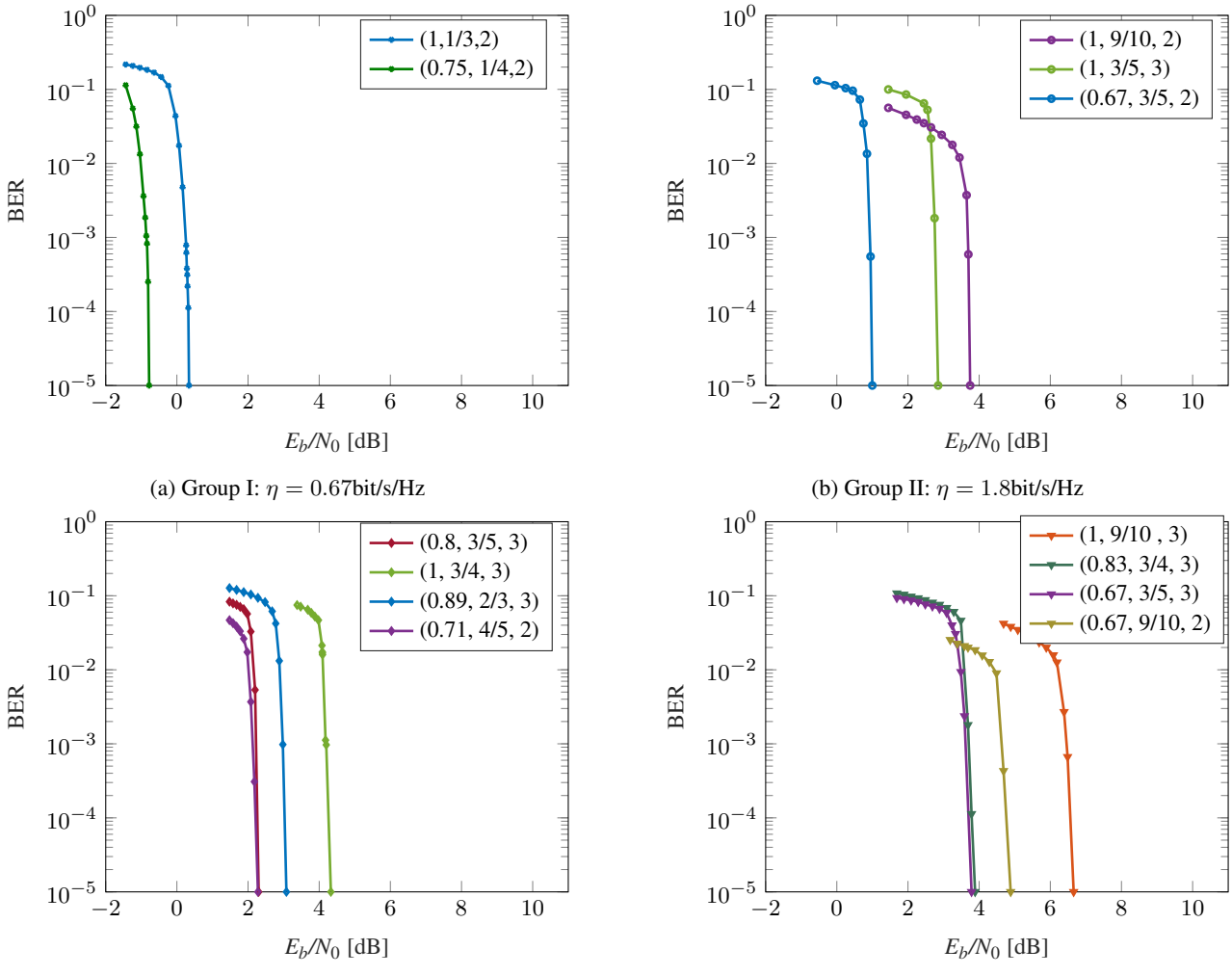

(a) Group I: $\eta = 0.67$bit/s/Hz

(b) Group II: $\eta = 1.8$bit/s/Hz

(c) Group III: $\eta = 2.25$bit/s/Hz

(d) Group IV: $\eta = 2.7$bit/s/Hz

Fig. 6: SEFDM system BER performance for the different QI groups with approach II receiver design and different VCCM parameters (α, R_c, $\log_2(M)$).

2.7bit/s/Hz). However, no enhancement is gained without a pay-off and ,in this case, it is the increase in detector complexity compared to approach I.

The results reported in this paper are based on system parameter adjustments to effect the same spectral efficiency values, in other words; the number of subcarriers was the same for all experiments (N=4) but the bandwidth and information bit rates were changed to maintain equal values of η. It is worth noting that the advantages of SEFDM can be also demonstrated when comparing systems of the same bandwidth but where the number of SEFDM subcarriers is increased relative to that of an OFDM system of the same spectral efficiency. For such scenarios, the number of required iterations will be increased but the error rates will be the same as those of Figs. 3 and 6. Such results are not reported here for reasons of space limitation.

6 Conclusions

This work investigates a proposal to increase the spectral efficiency of the design of high spectral efficiency satellite communication systems through the employment of a finite constellation SEFDM signals, coupled with LDPC channel coding and advanced interference cancellation processing via SIC turbo equalisation system. A special case for broadband and broadcasting applications (DVB-S2) is considered, where SEFDM provides more freedom in optimising the system, compared to orthogonal signals, by using VCCM.

In addition to the original single-user matched filter receiver with soft demapping (approach I), a turbo equaliser based on SIC (approach II) has been developed. The second approach overcomes the ICI problem and ameliorates its effects by subtracting the interference gradually.

The BER performance analysis are shown by system modelling and computer simulations to provide significant insight to these two approaches. A fair comparison is held by amending the bandwidth and information bit rates of SEFDM and OFDM signals to maintain the same spectral efficiency. Results show that SEFDM saves bandwidth compared to OFDM and requires less power while preserving the same BER performance. For high spectral efficiency values, interference cancellation becomes necessary to gain SEFDM advantages. For this purpose, the SIC method proposed shows its capability of reducing interference even with only one iteration.

SEFDM can be beneficial in another scenario that has not been detailed in this paper for brevity. This scenario increases the number of SEFDM subcarriers per transponder to maintain OFDM bandwidth rather than saving bandwidth for the same OFDM spectral efficiency. For such scenarios, the number of required iterations will be increased when the system is operating at relatively high spectral efficiency values, but for the same BER performance.

Finally, the analyses presented in this work allows the choice of an appropriate equalisation method for the given scenario. Our studies show that SIC is the most suitable method, as SIC is based on simple mathematical subtraction operation. Although there are compromises in terms of additional receiver complexity and added latency due to the iterations, the results of this work indicate possible new system design directions to improve further the spectral efficiency beyond what is used in today's FDM based DVB standards.

7 Acknowledgments

We are grateful to UCL for funding Hedaia Ghannam's PhD studies through the Overseas Research Student Award (ORS) and the UCL Dean of Engineering Sciences Award.

8 References

1 A. Piemontese, A. Modenini, G. Colavolpe, N. S. Alagha. "Improving The Spectral Efficiency of Nonlinear Satellite Systems through Time-Frequency Packing and Advanced Receiver Processing", *IEEE Trans. Commun.*, **61(8)**, pp. 3404–3412, (August 2013).

2 "Digital Video Broadcasting (DVB); Second Generation Framing Structure, Channel Coding and Modulation Systems for Broadcasting, Interactive Services, News Gathering and other Broadband Satellite Applications; Part 2: DVB-S2 Extensinos (DVB-S2X)", Technical report, European Standard (Telecommunications series), (10 2014).

3 A. Ugolini, Y. Zanettini, A. Piemontese, A. Vanelli-Coralli, G. Colavolpe. "Efficient Satellite Systems Based on Interference Management and Exploitation", *2016 50th Asilomar Conference on Signals, Systems and Computers, Pacific Grove.*, pp. 492–496, (Nov 2016).

4 T. Hwang, C. Yang, G. Wu, S. Li, G. Y. Li. "OFDM and Its Wireless Applications: A Survey", *IEEE Trans. Veh. Technol.*, **58(4)**, pp. 1673–1694, (May 2009).

5 J. Zhou, Y. Qiao, Z. Yang, M. Guo, X. Tang. "Capacity Limit for Faster-than-Nyquist Non-Orthogonal Frequency-Division Multiplexing Signaling", *Scientific Reports*, (2017).

6 J. Mazo. "Faster-than-Nyquist Signaling", *The Bell System Technical Journal*, **54(8)**, pp. 1451–1462, (Oct. 1975).

7 M. Rodrigues, I. Darwazeh. "A Spectrally Efficient Frequency Division Multiplexing Based Communications System", *Proc. 8th Int. OFDM Workshop, Hamburg*, pp. 48–49, (Nov. 2003).

8 F. Rusek, J. Anderson. "Multistream Faster than Nyquist Signaling", *IEEE Trans. Commun.*, **57(5)**, pp. 1329–1340, (May 2009).

9 J. B. Anderson, F. Rusek, V. Öwall. "Faster-than-Nyquist Signaling", *Proc. IEEE*, **101(8)**, pp. 1817–1830, (Aug 2013).

10 A. Barbieri, D. Fertonani, G. Colavolpe. "Time-Frequency Packing for Linear Modulations: Spectral Efficiency and Practical Detection Schemes", *IEEE Trans. Commun.*, **57(10)**, pp. 2951–2959, (October 2009).

11 P. N. Whatmough, M. R. Perrett, S. Isam, I. Darwazeh. "VLSI Architecture for a Reconfigurable Spectrally Efficient FDM Baseband Transmitter", *IEEE Trans. Circuits Syst. I, Reg. Papers*, **59(5)**, pp. 1107–1118, (May 2012).

12 I. Kanaras, A. Chorti, M. R. D. Rodrigues, I. Darwazeh. "Spectrally Efficient FDM Signals: Bandwidth Gain at the Expense of Receiver Complexity", *Proc. IEEE Int. Conf. Commun. (ICC) Dersen.*, pp. 1–6, (June 2009).

13 T. Xu, I. Darwazeh. "Transmission Experiment of Bandwidth Compressed Carrier Aggregation in a Realistic Fading Channel", *IEEE Trans. Veh. Technol.*, (2016).

14 T. Xu, S. Mikroulis, J. E. Mitchell, I. Darwazeh. "Bandwidth Compressed Waveform for 60-GHz Millimeter-Wave Radio over Fiber Experiment", *J. of Lightwave Technol.*, **34(14)**, pp. 3458–3465, (July 2016).

15 D. Nopchinda, T. Xu, R. Maher, B. C. Thomsen, I. Darwazeh. "Dual Polarization Coherent Optical Spectrally Efficient Frequency Division Multiplexing", *IEEE Photon. Technol. Lett*, **28(1)**, pp. 83–86, (Jan 2016).

16 S. Isam, I. Darwazeh. "Peak to Average Power Ratio Reduction in Spectrally Efficient FDM Systems", *2011 18th Int. Conf. on Telecom., Cyprus.*, pp. 363–368, (May 2011).

17 "Digital Video Broadcasting (DVB); Second Generation Framing Structure, Channel Coding and Modulation Systems for Broadcasting, Interactive Services, News Gathering and Other Broadband Satellite Applications (DVB-S2)", Technical report, European Standard (Telecommunications series), (08 2009).

18 C. Berrou, A. Glavieux, P. Thitimajshima. "Near Shannon Limit Error-Correcting Coding and Decoding: Turbo-codes. 1", *IEEE Int. Conf. on Comm., 1993. ICC '93 Geneva.*, volume 2, pp. 1064–1070 vol.2, (May 1993).

19 C. Douillard, M. Jézéquel, C. Berrou, D. Electronique, A. Picart, P. Didier, A. Glavieux. "Iterative Correction of Intersymbol Interference: Turbo-Equalization", *European Trans. Telecommun.*, **6(5)**, pp. 507–511, (1995).

20 M. Tuchler, R. Koetter, A. C. Singer. "Turbo Equalization: Principles and New Results", *IEEE Trans. Commun.*, **50(5)**, pp. 754–767, (May 2002).

21 X. Wang, H. V. Poor. "Iterative (turbo) Soft Interference Cancellation and Decoding for Coded CDMA", *IEEE Trans. Commun.*, **47(7)**, pp. 1046–1061, (Jul 1999).

22 A. F. Molisch, M. Toeltsch, S. Vermani. "Iterative Methods for Cancellation of Intercarrier Interference in OFDM Systems", *IEEE Trans. Veh. Technol.*, **56(4)**, pp. 2158–2167, (July 2007).

23 T. Xu, I. Darwazeh. "Nyquist-SEFDM: Pulse Shaped Multicarrier Communication with Sub-carrier Spacing below the Symbol Rate", *Proc. 10th Int. Symp. Commun. Syst. Networks and Digital Signal Process. (CSNDSP), Prague.*, pp. 1–6, (July 2016).

24 T. Xu, I. Darwazeh. "Bandwidth Compressed Carrier Aggregation", *2015 IEEE Int. Conf. on Commun. Workshop (ICCW), London.*, pp. 1107–1112, (June 2015).

25 A. Morello, V. Mignone. "DVB-S2: The Second Generation Standard for Satellite Broad-Band Services", *Proc. IEEE*, **94(1)**, pp. 210–227, (Jan 2006).

26 S. Isam, I. Darwazeh. "Characterizing the Intercarrier Interference of Non-orthogonal Spectrally Efficient FDM System", *2012 8th International Symposium on Communication Systems, Networks Digital Signal Processing (CSNDSP), Poznan*, pp. 1–5, (July 2012).

27 B. F. Beidas, R. I. Seshadri, N. Becker. "Multicarrier Successive Predistortion for Nonlinear Satellite Systems", *IEEE Trans. Commun.*, **63(4)**, pp. 1373–1382, (April 2015).

28 B. F. Beidas, H. E. Gamal, S. Kay. "Iterative Interference Cancellation for High Spectral Efficiency Satellite Communications", *IEEE Trans. Commun.*, **50(1)**, pp. 31–36, (Jan 2002).